# Supporting Information

## Selective Nucleation and Growth of Cu and Ni Core-Shell Nanoparticles

Kyler J. Carroll[†], Scott Calvin[#], Thomas F. Ekiert[‡], Karl M. Unruh[‡], Everett E. Carpenter[†]

*Department of Chemistry, Virginia Commonwealth University, Richmond VA 23284, Department of Physics, Sarah Lawrence College, 1 Mead Way, Bronxville NY 10708, Department of Physics and Astronomy, University of Delaware, Newark, DE 19716*

**Materials.** Copper (II) chloride dihydrate ($CuCl_2 \cdot 2H_2O$), nickel (II) chloride hexahydrate ($NiCl_2 \cdot 6H_2O$), and sodium hydroxide (NaOH) were all purchased from Fisher. Ethylene glycol (EG) was purchased from Acros Organics. All chemicals were used as received.

**Synthesis of Cu-Ni CSNPs.** Approximately 0.5 g $CuCl_2 \cdot 2H_2O$, 0.5 g $NiCl_2 \cdot 6H_2O$, and 3 M NaOH were dissolved in 25 mL of EG. The solution was refluxed for 30 to 60 minutes. Following reflux, a distillation apparatus was attached to the boiling solution for an additional 30 to 60 minutes. After cooling to room temperature, the precipitate was isolated by magnetic extraction, washed several times with methanol, and vacuum dried.

**Synthesis of Ni-Cu CSNPs.** Approximately 0.5 g $NiCl_2 \cdot 6H_2O$ and 3 M NaOH were dissolved in 25 mL of EG. The solution was distilled for 30 to 60 minutes to fully reduce the Ni. In a separate flask, 0.5 g $CuCl_2 \cdot 2H_2O$ was dissolved in 25 mL of EG and added to the Ni solution. The solution was then heated to reflux for 60 minutes. The particles were magnetically separated, washed several times with methanol, and vacuum dried.

**Synthesis of pure Ni and Cu nanoparticles.** Elemental Ni and Cu nanoparticles were prepared by refluxing a $CuCl_2 * 2H_2O$/EG/NaOH solution and distilling a $NiCl_2 * 2H_2O$/EG/NaOH solution according to the procedures described above.

**Characterization of CSNPs.** Transmission electron microscopy (TEM) images and elemental composition maps were taken on a JEOL JEM-3010 transmission electron microscope equipped with an EDX EDS detector. The TEM samples were prepared by evaporating a small quantity of the CSNPs suspended in acetone onto a Formvar/carbon 200 mesh copper grid. The x-ray diffraction (XRD) measurements were carried out on a Panalytical X'Pert Pro powder diffractometer using $CuK_\alpha$ radiation. The hysteresis loop measurements were carried out at room temperature on a Lakeshore model 7300 vibrating sample magnetometer (VSM). The measuring field was oriented parallel to the plane of the sample disk. Elemental compositions of the CSNPs were determined using a Varian Vista-MPX CCD inductively coupled plasma - optical emission spectrometer (ICP-OES). Samples were prepared by nitric acid digestion.

X-ray absorption spectroscopy (XAS) measurements at the copper and nickel K edge of the Ni/Cu CSNPs were carried out at the National Synchrotron Light Source on beamline X-11B. Samples were prepared by spreading thin layers of finely ground as-prepared powders on multiple layers of Kapton tape. The number of layers was chosen to make the absorption edge jumps approximately 0.44 at the copper edge and 0.76 at the nickel edge. After detuning the channel-cut monochromator by about 25% before measuring each edge, a total of 27 scans at the nickel edge and 4 scans at the copper edge were averaged (the larger number of nickel scans was due to an overnight run and does not reflect the relative quality of the Cu and Ni edge measurements); corresponding pure metal foils were also measured in a reference channel. The XAS spectra were analyzed using the Ifeffit and Horae software packages.[1] The extended x-ray absorption fine structure (EXAFS) region of the spectra were fit to *ab initio* theoretical standards.[2]

Background subtraction for each edge was performed using the method of Newville with a cut-off frequency for the background spline of 1.0 Å and a normalization correction based on the data of McMaster.[3] This data was transformed to a function of photoelectron wavenumber $k$ and multiplied by $k^3$ (see Figure S1). The Fourier transform of the data over a range of 3.0 – 12.0 $Å^{-1}$ was then taken using Hanning windows with sills of size 1.0 $Å^{-1}$ and compared with theoretical standards calculated using Feff6L.[4] The first 7 direct scattering paths and 34 associated multiple-scattering paths were incorporated in the copper theoretical standard; 7 direct scattering paths and 37 associated multiple-scattering paths were incorporated in the nickel theoretical standard. These standards were fit to the data, as well as data collected from the reference foils, over the range of 1.2 to 5.0 Å, yielding 22 independent points for each edge according to the Nyquist criterion. Because the copper edge is less than 700 eV above the nickel edge, nickel edge EXAFS contributes to the signal in the copper EXAFS region. To account for this, the nickel edge was fit first, and then the results used to constrain the contribution of nickel absorption to the copper edge. Fits to the metal foils were corefined with fits to the sample, both for purposes of comparison and to allow an improved determination of the EXAFS amplitude reduction factor ($S_o^2$) and the photoelectron energy origin ($E_o$).

For each edge four parameters were fit for the sample, three for the reference, and two ($S_o^2$ and $E_o$) which apply to both sample and reference. The parameters fit separately for sample and reference were the lattice parameter, Debye temperature, and the EXAFS third cumulant (a measure of the asymmetry of the pair distribution function).[5] The additional parameter used for the sample was the crystallite size under the spherical homogenous model,[6] which provides a measure of the scale of crystallinity but can be much smaller than the physical particle size. For each edge this number of parameters gives 22 x 2 – (4 + 3 + 2) = 35 degrees of freedom in the fit. The results of these fits are given in Figure S2 and Table S1. The R – factor, given in the bottom row of the table, is widely used in the EXAFS community as a measure of closeness of fit. An R – factor of zero would indicate a perfect match between fit and data; values below 0.02 are often considered to be "good" fits in the sense of matching the data well.

EXAFS analysis confirms that essentially all the copper and nickel are present as fcc metals (Figure S2). The slight changes in the lattice parameters suggest a small degree of alloying, with the copper lattice parameter for the sample slightly lower than the corresponding foil, and the nickel lattice parameter somewhat higher (Table S1). Depending on the morphology of the core/shell boundary, this may simply represent the boundary layer between the two phases. EXAFS is known to yield characteristic crystallite sizes weighted toward the smallest features present, therefore, a crystallite radius of about 10 Å is consistent with the measured crystallite size determined from the Scherrer equation (Table S2).[7]

**Table S1**. EXAFS fitting parameters and resulting lattice parameters of the copper edge and nickel edge of the Ni/Cu CSNPs, and their respective foil fits.

| | Cu edge: sample | Cu edge: foil | Ni edge: sample | Ni edge: foil |
|---|---|---|---|---|
| $S_o^2$ | 1.02(5) | | 0.92(4) | |
| $E_o$ | 8986.7(5) eV | | 8341.1(5) eV | |
| Lattice parameter | 3.623(5) Å | 3.628(4) Å | 3.534(6) Å | 3.528(4) Å |
| Debye temperature | 321(8) K | 316(6) K | 401(13) K | 394(9) K |
| Third cumulant | 0.00026(5) Å$^3$ | 0.00023(4) Å$^3$ | 0.00016(6) Å$^3$ | 0.00013(3) Å$^3$ |
| Crystallite radius | 10(2) Å | --- | 10(2) Å | --- |
| $\mathcal{R}-$ factor | 0.008 | 0.007 | 0.005 | 0.006 |

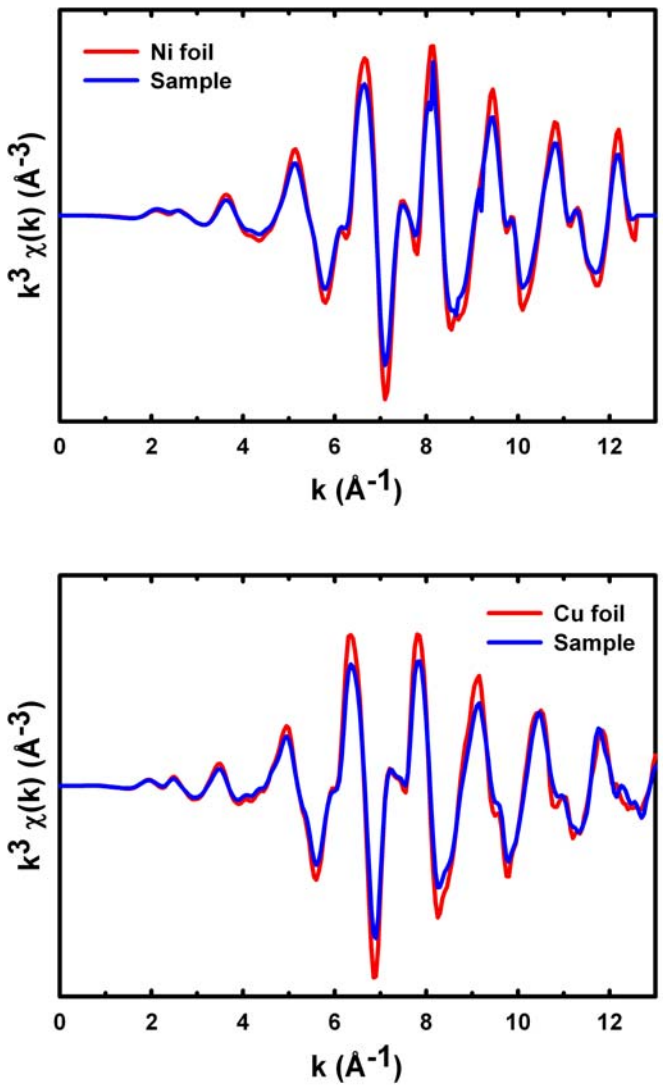


**Figure S1**. Ni (top) and Cu (bottom) EXAFS spectra of Ni/Cu CSNPs and the metal foils.

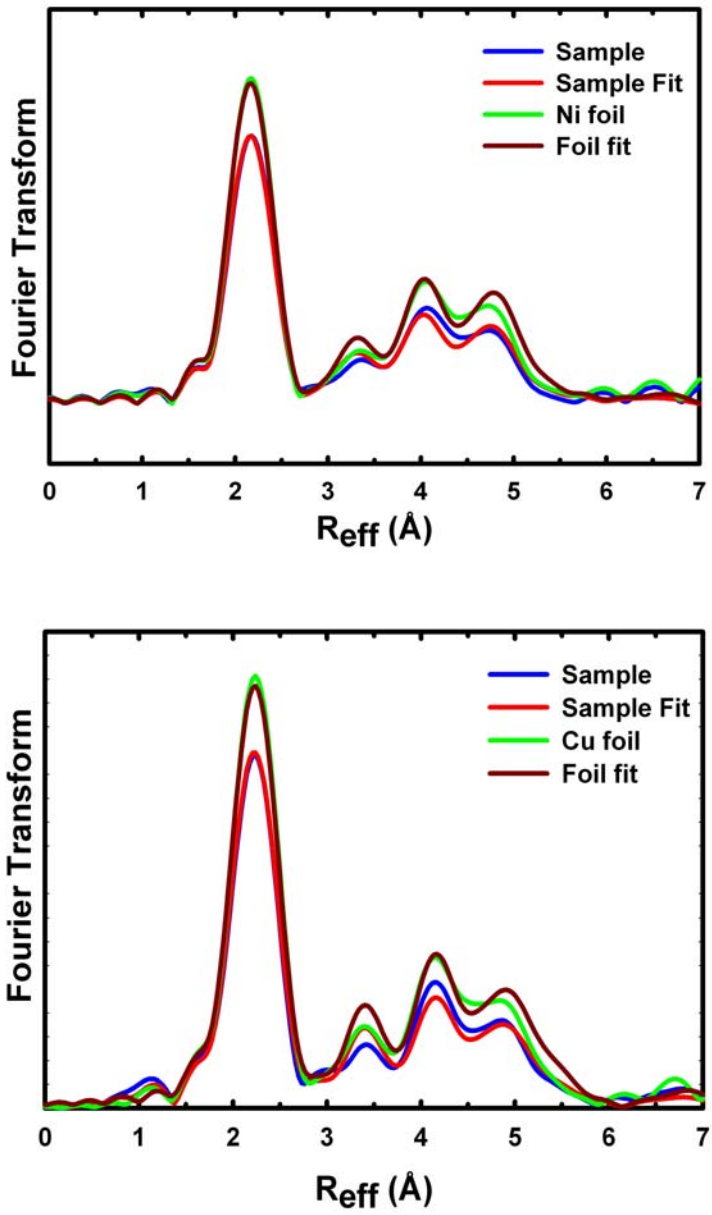


**Figure S2.** Fourier transform of the EXAFS signals from Ni (top) and Cu (bottom) in the Ni/Cu CSNPs with their fits, along with corresponding foils and their fit.

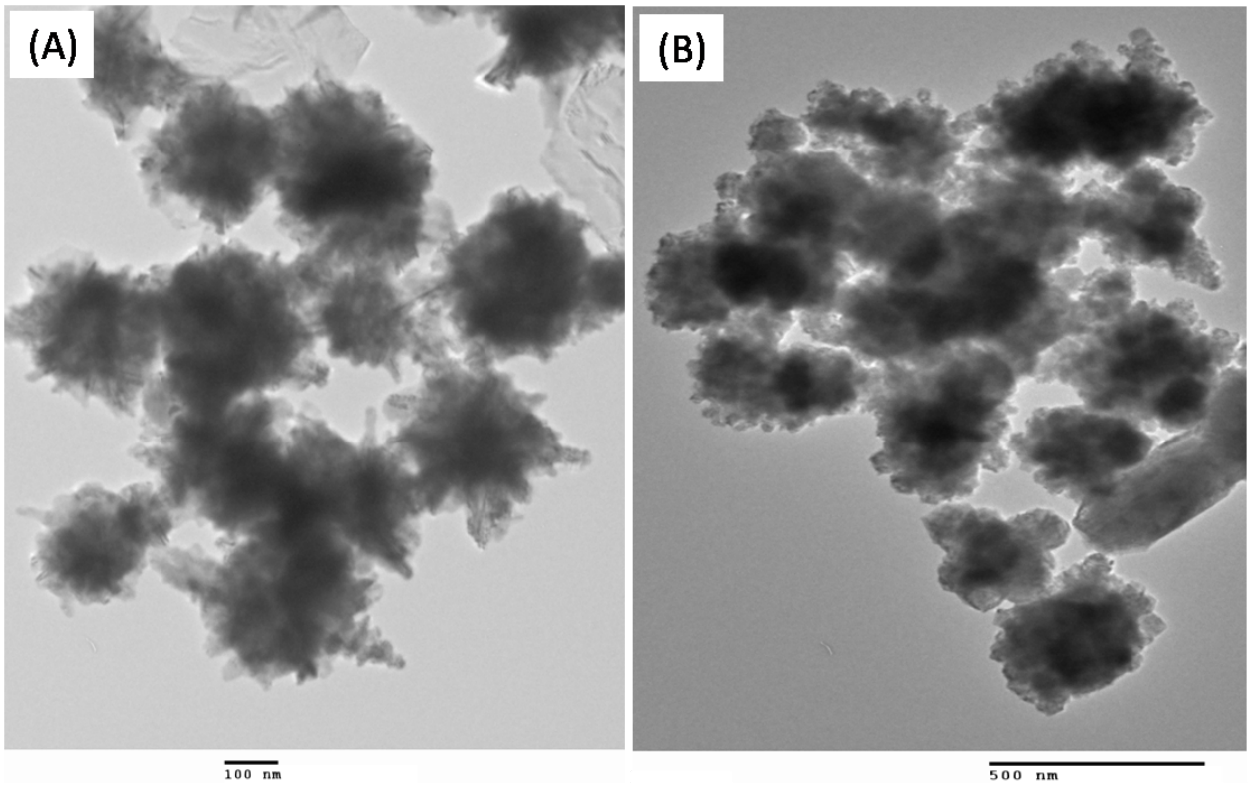


**Figure S3.** TEM images of the Cu/Ni (A) and Ni/Cu (B) CSNPs showing the particle size distribution.

**References**

(1) (a) Newville, M., *J. Synchrotron Rad.* **2001,** 8, 322-324;(b) Ravel, B.; Newville, M., *J.Synchrotron Rad.* **2005,** 12, (4), 537-541.
(2) Rehr, J. J.; Albers, R. C., *Rev. Mod. Phys.* **2000,** 72, 621-654.
(3) (a) McMaster, W. H.; Grande, N. K. d., et al., *Lawrence Livermore National Laboratory Report* **1969,** UCRL-50174;(b) Newville, M.; Livins, P., et al., *Phys. Rev. B* **1993,** 47, 14126-14131.
(4) Rehr, J. J.; Zabinsky, S. I., et al., *Phys. Rev. Lett.* **1992,** 69, 3397.
(5) Hung, N. V.; Rehr, J. J., *Phys. Rev. B* **1997,** 56, 43-46.
(6) Calvin, S.; Miller, M. M., et al., *J. Appl. Phys.* **2003,** 94, 778-783.
(7) Calvin, S.; Luo, S. X., et al., *Appl. Phys. Lett.* **2005,** 87, 233102.